Available online at www.sciencedirect.com
ScienceDirect
Journal of Hazardous Materials 140 (2007) 361–368
Journal of Hazardous Materials
www.elsevier.com/locate/jhazmat

Thin-layer boilover in diesel-oil fires: Determining the increase of thermal hazards and safety distances

Fabio Ferrero *, Miguel Muñoz, Josep Arnaldos

Centre d'Estudis del Risc Tecnològic (CERTEC), Chemical Engineering Department, Universitat Politècnica de Catalunya, Diagonal 647, 08028 Barcelona, Catalonia, Spain

Received 14 June 2006; received in revised form 19 September 2006; accepted 20 September 2006
Available online 26 September 2006

Abstract

A study of the effects of thin-layer boilover on large hydrocarbon fires was carried out. In the experiments, diesel-oil was burned in pools with diameters ranging from 1.5 to 6 m. Previous models used to predict emissive power during the stationary state were analysed and successively modified in order to accurately predict thermal hazard during the water ebullition phase. It was discovered that the increase in emissive power during thin-layer boilover is greater when the pool diameter is smaller. Furthermore, the required increases in safety distances in the case of accidents involving this dangerous phenomenon are provided.

Keywords: Pool fire; Thin-layer boilover; Thermal hazards; Safety distances

1. Introduction

Thermal hazard assessment is without doubt the most important precaution when one is considering pool fires and there are a great number of studies dealing with this matter [1–6]. Accidental fires frequently involve a hydrocarbon burning above a water layer, creating a situation in which boilover can occur. In fact, when the fuel boiling temperature exceeds that of water, heat transfer from the flame can lead to violent-eruptive vaporisation of the water layer, resulting in the ejection of burning fuel and an increase in the turbulence of the fire, in turn increasing flame size and radiation.

Although the increase in thermal hazard during boilover is a well known phenomenon, there is little quantitative information and it is difficult to find equations to predict such increases in the literature. The aim of this work is to provide a tool for estimating thermal radiation during thin-layer boilover and to present a series of safety distances to be applied. Even if the effects of a hot zone boilover – often referred to simply as boilover – are more disruptive, this work was directed to thin-layer boilover, since the impact in term of radiation is still important. In [7,8] discussions about the two type of boilover are given.

It should also be noted that thin-layer boilover has been studied mainly on a laboratory scale [9–12]. The results obtained from the present study are therefore even more representative, since the experiments were performed in pools with diameters ranging from 1.5 to 6 m.

Note that, unless otherwise stated, the term "boilover" shall be used in the rest of the paper to refer to thin-layer boilover.

2. Experimental facility

Two commercial hydrocarbons were used for the experiments: gasoline REPSOL 98, unleaded, and diesel-oil REPSOL, C type. A total of 22 experiments were performed. This study deals exclusively with the 15 diesel-oil experiments, as this was the only fuel to exhibit boilover. Five concentric circular pools made of reinforced concrete (with diameters of 1.5, 3, 4, 5 and 6 m) were used. The facility was designed to measure the maximum number of fire properties. In order to determine flame temperatures, thermocouples were fixed at different positions on a metal structure built on a concrete base set 1 m from the outer pool. The temperature of the two fuel and water phases and the fuel/water interface was measured using another 10 thermocouples of K-type, fixed on the pool axis at a distance of 2 mm

* Corresponding author. Tel.: +34 93 401 66 75; fax: +34 93 401 71 50.
E-mail address: fabio.ferrero@upc.edu (F. Ferrero).

0304-3894/$ – see front matter © 2006 Elsevier B.V. All rights reserved.
doi:10.1016/j.jhazmat.2006.09.062

Nomenclature

D	pool diameter (m)
E	average emissive power of the flame (kW/m^2)
F	view factor between flame and target
g	gravity acceleration (m/s^2)
h_b	fuel thickness at boilover on-set (mm)
$I_{b,rad}$	radiation intensity
$\dot{m}$	burning rate (kg m^{-2} s^{-1})
$\dot{q}$	heat flux received by a target at certain distance from the pool (kW/m^2)
T_l	flame temperature (K)
u	wind speed (m/s)
u_c	characteristic burning rate (m/s)

Greek letters

ε	flame emissivity
ρ_a	air density (kg/m^3)
σ	Stefan–Boltzmann constant (5.67×10^{-8} W m^{-2} K^{-4})
τ	atmospheric transmissivity

Statistical parameter

NMSE	normalised mean square error
FB	fractional bias

Subscripts

b	boilover
s	stationary

one from another. The tests were also recorded with two video cameras, in order to study the flame height, and with a thermographic camera (IR). These cameras were accurately fixed so that the flames could be viewed in their entirety. The burning rate was determined by measuring the variation in the fuel level with a system of communicating vessels. The increase in the sound level of the fire during boilover was used to detect the start of the phenomenon [13]. Two heat flux sensors were employed to measure the external radiation on a target at specified distances. Meteorological parameters that could affect the development of the fire – particularly wind speed – were continuously monitored. All data was collected on computer without loss of synchronisation using a specially developed data acquisition software package.

Further details on the experimental set-up and procedures can be found in [14,15].

3. Results

3.1. Radiation intensity

One of the ways of measuring the effects of boilover is through the radiation intensity, as defined by Koseki [7]. Radiation intensity is the increase during boilover – with respect to the stationary period – in radiation emitted from the flame and received by a target located at a certain distance from the fire. It is expressed by Eq. (1):

$$I_{b,rad} = \frac{\dot{q}_b}{\dot{q}_s} \quad (1)$$

Average heat fluxes during the stationary and boilover phases and the resulting radiation intensities are shown in Table 1. It has to be noticed that, since thin-layer boilover is a phenomenon with certain duration [13], the heat flux during boilover is an average during this period and the maximum value like in [7]. Although little previous data is available for thin-layer boilover, the values are of the same order of magnitude as the experiments of Koseki [7], with 30 mm of crude-oil as fuel.

In [13] it was observed that the thickness of the remaining fuel at the onset of boilover is the limiting factor of boilover intensity, a parameter that expresses the effects of boilover on burning rate. In accordance with this observation, Fig. 1 shows radiation intensity against the fuel thickness at the boilover onset, for every pool diameter. Radiation intensity increases according to the quantity of fuel remaining at the onset of boilover. This means that if fuel thickness at the onset of boilover tends to decrease with the diameter radiation intensity also decreases with diameter. This trend can also be observed in [7].

3.2. Choice of model

In fire hazard assessments, it is common to use the solid flame model. This consists of assimilate the flame to a simple surface, usually a cone or a cylinder, and determining the radiation that hits targets, using Eq. (2):

$$\dot{q} = \tau E F \quad (2)$$

This means that the heat flux on a target $\dot{q}$ is calculated as product of the atmospheric transmissivity, τ, the average emissive power of the flame, E, and the view factor between flame and target, F.

Atmospheric transmissivity represents the capacity of air to absorb radiation and essentially depends on relative humidity,

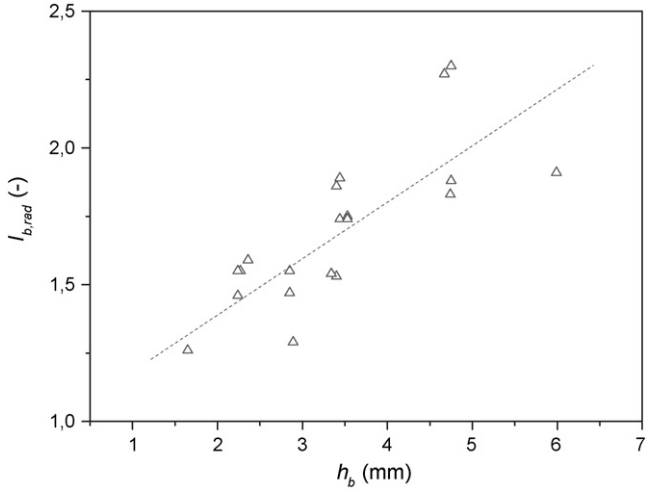

Fig. 1. Radiation intensity vs. fuel thickness at the boilover onset.

Table 1
Average heat fluxes and radiation intensity in the experiments performed

Experiment	D (m)	h_0 (mm)	h_b (mm)	x_c/D	$\dot{q}_s$ (kW/m^2)	$\dot{q}_b$ (kW/m^2)	$I_{b,rad}$
FOC3_22_D1.5	1.5	19.8	5.99	5.00	1.61	3.07	1.91
FOC3_01_D3	3	12.7	4.74	3.00	3.53	6.46	1.83
FOC3_02_D3	3	15.0	3.53	5.00	1.01	1.77	1.75
FOC3_02_D3	3	15.0	3.53	5.00	1.04	1.81	1.74
FOC3_04_D3	3	20.1	4.67	5.00	1.05	2.39	2.27
FOC3_05_D3	3	24.9	4.75	5.33	1.27	2.39	1.88
FOC3_05_D3	3	24.9	4.75	7.33	0.47	1.08	2.30
FOC3_18_D3	3	12.0	3.40	3.00	4.86	7.42	1.53
FOC3_18_D3	3	12.0	3.40	5.00	1.30	2.42	1.86
FOC3_20_D3	3	12.0	3.44	3.00	4.08	7.11	1.74
FOC3_20_D3	3	12.0	3.44	5.00	2.90	5.50	1.89
FOC3_14_D4	4	15.0	2.27	3.00	3.11	4.82	1.55
FOC3_15_D4	4	20.0	2.89	3.00	4.74	6.13	1.29
FOC3_15_D4	4	20.0	2.89	5.00	1.49	1.91	1.29
FOC3_16_D4	4	25.0	1.90	3.00	3.12	6.43	2.06
FOC3_16_D4	4	25.0	1.90	5.00	1.15	2.13	1.86
FOC3_09_D5	5	15.0	3.34	3.00	2.48	3.81	1.54
FOC3_10_D5	5	20.0	2.85	3.00	3.31	5.13	1.55
FOC3_10_D5	5	20.0	2.85	5.00	0.97	1.43	1.47
FOC3_11_D5	5	20.4	1.65	3.00	4.01	5.07	1.26
FOC3_11_D5	5	20.4	1.65	5.00	1.21	1.53	1.26
FOC3_07_D6	6	15.0	2.36	3.00	2.21	3.52	1.59
FOC3_12_D6	6	20.0	2.24	3.00	2.46	3.83	1.55
FOC3_12_D6	6	20.0	2.24	5.00	0.80	1.17	1.46

ambient temperature and the distance between the flame surface and target. Of the various equations proposed for the estimation of this parameter, the suggestions made by Bagster and Pitblado [16] and Wayne [17] were used. Note that, for the definition of transmissivity, these correlations are applicable in both the stationary and boilover phases of the fire.

Emissive power is defined as the thermal radiation emitted by a body towards a target per unit of time and surface. A flame is made up of a group of points, each one with a different emissive power that can by determined by the Stefan–Boltzmann law:

$$E(i, j) = \varepsilon\sigma T_l^4(i, j) \tag{3}$$

In large hydrocarbon fires, the parts of the flame that contribute to radiation emission are essentially the continuous flame zone and the intermittent flame zone, since the emissions of a fire plume are usually negligible due to low temperatures. The average flame emissive power will therefore depend on the dimensions of these two zones. The lower part (continuous flame) has

Table 2
General overview of the models used to determine the emissive power of the flame

Model	Reference	Fuels	Description
E-SHOKRI	[1]	Previous experimental results	This model predicts an emissive power that decreases exponentially with pool diameter, according to the increase in smoke production
E-MUDAN	[2]	Diesel-oil, kerosene and JP5	This model predicts an emissive power between that of the luminous flame (140 kW/m^2) and that of the non-luminous flame (20 kW/m^2), the values always decreasing with pool diameter
E-REW_MOD	[3,4]	Previous experimental results	The model considers that portions of luminous flame can also appear in the upper part of the flame. The height of the lower part decreases with the diameter. The original two zone model is converted to a single zone model with an average emissive power between the two zones
E-TNO/EFFECTS	[5]		This model uses a fraction of energy irradiation equal to 0.35 to estimate the maximum emissive power of the flame, which also depends on the diameter. The average emissive power is then valued between this maximum and the emissive power of soot (20 kW/m^2)
E-MUÑOZ	[6]	Gasoline, diesel-oil	This model predicts an emissive power between that of the luminous flame and that of the non-luminous flame (soot), according to the fraction occupied by smoke. Both the occupied fraction and the luminous emissive power change with the diameter, while for soot a value of 40 kW/m^2 is assigned
E-FRAC_RAD	[6,15]	Gasoline, diesel-oil	This model uses a fraction of energy irradiation that varies with the diameter to calculate the average emissive power of the flame. The values increase up to 4 m and then show a sudden decrease

a very high emissive power (around 120–140 kW/m^2), while the higher part (intermittent flame) is often partially obscured by smoke and is assigned an emissive power of 20–40 kW/m^2. Table 2 gives a brief description of the correlations chosen in our analysis to estimate the average emissive power of large hydrocarbon fires during the stationary period. Since, as it was observed experimentally in all the diesel fires, the amount of smoke is reduced during boilover, it is reasonable to assume that the average emissive power will increase. The aim of this work is to quantify such an increase in order to obtain reliable values on which to base requirements for safety distances in the case of accidents involving thin-layer boilover.

The view factor between flame and object is defined as the ratio between the radiation emitted by the flame and that which directly (without reflection) hits the object. This parameter is entirely geometric and, as such, varies according to the shape of the flame selected. In order to determine the view factor between finite surfaces, it is necessary to use a double integration that can prove extremely laborious when the shapes are irregular. Nevertheless, for the most common geometries, pre-calculated view factors can be found in the literature. In this study – as can be seen in the video recording of the experiments – a cylindrical flame was used, either straight or tilted depending on whether the fire developed without or with wind. It should be noted that the heat flux sensors were placed upwind in all experiments performed, in case of presence of wind. The view factor formulae given in [18] were used for both the straight and tilted cylinder.

The flame length and, consequently, the view factor increase during boilover. Thus, the increase of radiation during boilover is caused by two factors: the increase of the view factor and the rise in emissive power.

Through the definition of radiation intensity, $I_{b,rad}$, and taking into account Eq. (2), it is possible to express:

$$I_{b,rad} = \frac{\dot{q}_b}{\dot{q}_s} = \frac{\tau E_b F_b}{\tau E_s F_s} = \frac{E_b F_b}{E_s F_s} \quad (4)$$

where sub-indexes b and s refer to the boilover and stationary periods, respectively. The view factors F_b and F_s can easily be determined when the flame length and tilt are known. The average emissive power in the steady state E_s is determined from previous correlations in the literature. Therefore, since the values of $I_{b,rad}$ were calculated from the experimental measurement of $\dot{q}_b$ and $\dot{q}_s$, the average emissive power during boilover E_b can be estimated.

In order to determine flame length and tilt angle for both the stationary and boilover periods, the correlations established from the experimental data were used; these correlations are given in [19]. The resulting view factors are shown in Table 3. Note that in some cases, since the inclination of the flame was greater during boilover, the value given may be lower than in the stationary phase.

Because of the large number of possible equations for predicting the emissive power of the flame during the stationary period, a study was carried out in order to determine which of them presented the smallest deviations from the experimental values. In order to perform this analysis, two statistical parameters were employed: the normal mean square error (NMSE) and the fractional bias (FB), defined as

$$\mathrm{NMSE} = \frac{1}{n}\sum_{1}^{n}\frac{(x_0 - x_p)^2}{x_0 x_p} \quad (5)$$

Table 3
View factors in the experiments

Experiment	D (m)	x_c/D	u_s (m/s)	u_b (m/s)	F_s[a]	F_b[a]
FOC3_22_D1.5	1.5	5.00	0.80	0.71	0.037	0.036
FOC3_01_D3	3	3.00	1.62	2.28	0.100	0.102
FOC3_02_D3	3	5.00	1.75	1.37	0.023	0.030
FOC3_02_D3	3	5.00	1.75	1.37	0.023	0.030
FOC3_04_D3	3	5.00	0.00	0.39	0.029	0.033
FOC3_05_D3	3	5.33	0.51	0.41	0.027	0.033
FOC3_05_D3	3	7.33	0.51	0.41	0.015	0.018
FOC3_18_D3	3	3.00	1.32	1.00	0.117	0.118
FOC3_18_D3	3	5.00	1.32	1.00	0.038	0.046
FOC3_20_D3	3	3.00	0.86	0.22	0.080	0.072
FOC3_20_D3	3	5.00	0.86	0.22	0.033	0.033
FOC3_14_D4	4	3.00	0.81	0.64	0.066	0.071
FOC3_15_D4	4	3.00	1.65	1.05	0.108	0.073
FOC3_15_D4	4	5.00	1.65	1.05	0.035	0.030
FOC3_16_D4	4	3.00	0.79	1.45	0.076	0.118
FOC3_16_D4	4	5.00	0.79	1.45	0.030	0.041
FOC3_09_D5	5	3.00	0.57	0.62	0.065	0.070
FOC3_10_D5	5	3.00	1.35	2.08	0.064	0.056
FOC3_10_D5	5	5.00	1.35	2.08	0.025	0.022
FOC3_11_D5	5	3.00	1.96	1.50	0.095	0.111
FOC3_11_D5	5	5.00	1.96	1.50	0.030	0.038
FOC3_07_D6	6	3.00	0.81	0.75	0.065	0.067
FOC3_12_D6	6	3.00	0.20	1.15	0.065	0.081
FOC3_12_D6	6	5.00	0.20	1.15	0.029	0.034

[a] Values obtained using maximum flame length equations.

Table 4
Comparison between various combinations of the different equations of atmospheric transmissivity and average emissive power

Model	E	τ	NMSE	FB
1	E-SHOKRI	Wayne [17]	0.106	−0.171
2	E-MUÑOZ	Wayne [17]	0.138	−0.183
3	E-FRAC_RAD	Wayne [17]	0.149	0.219
4	E-REW_MOD	Wayne [17]	0.152	0.248
5	E-TNO/EFFECTS	Wayne [17]	0.270	0.394
6	E-MUDAN	Wayne [17]	0.665	−0.697
7	E-REW_MOD	1	0.077	0.180
8	E-FRAC_RAD	1	0.073	0.137
9	E-SHOKRI	Bagster and Pitblado [16]	0.044	−0.064
10	E-MUÑOZ	Bagster and Pitblado [16]	0.065	−0.076

$$\mathrm{FB} = \frac{1}{n}\sum_{1}^{n} 2\frac{x_0 - x_\mathrm{p}}{x_0 + x_\mathrm{p}} \tag{6}$$

where x_0 and x_p are the experimental and calculated values, respectively. NMSE measures the accuracy of the correlation: the closer to 0, the better the correlation. By contrast, FB gives the degree of deviation: a negative value means that the correlation overestimates the experimental values, while a positive value indicates an underestimation.

Results are shown in Table 4. As stated, maximum flame length values were used in the calculations, since most of the emissive power models were also determined in this way. As a first approximation, Wayne's formula for τ determination was used for all the selected models (models 1–6). Table 4 shows that the values given by models 5 and 6 differ greatly from the experimental data; in fact, model 5 dramatically underestimates the data, while model 6 gives an overestimation. Consequently, these two models were immediately discarded.

In all other cases, the models were enhanced by the use of other values of atmospheric transmissivity. For models using the equations of E-REW_MOD and E-FRAC_RAD – which underestimate the experimental data – the value of τ was always equal to 1, giving a reasonable increase in accuracy. For models employing the equations proposed by E-SHOKRI and E-MUÑOZ, Bagster and Pitblado's formula for τ gave the smallest deviation from the experimental data.

Models 7–10 offer reasonable approximations of experimental heat fluxes in the stationary period. Consequently, the emissive power during boilover, E_b, from Eq. (4), was calculated for all of these cases before selecting the most adequate.

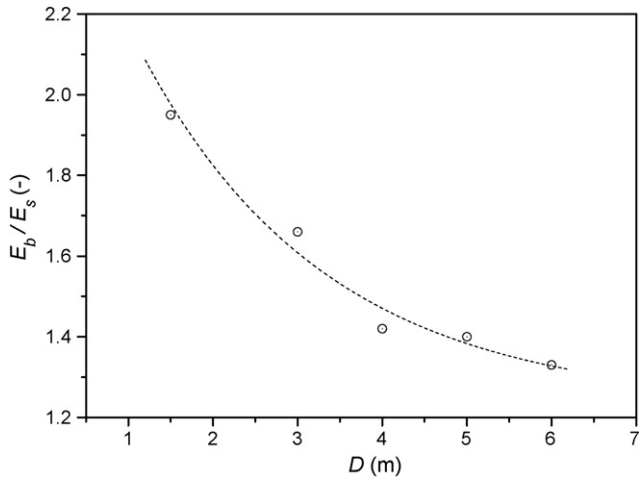

Fig. 2. Ratio between average emissive power during boilover and stationary as a function of diameter.

For each model, values of E_s and E_b were determined in all the experiments and were then averaged with diameter (Table 5). Due to the strong influence of wind on heat flux sensor measurements, only those fires in which the wind speed was lower than 1.5 m/s were included when calculating averages; this value, selected by observing the fluctuation in the values of E_b, had already been used as the limit for measurements of burning rate in previous studies with the same experiments [14,15].

By examining Table 5, it can be seen that even if the four models give heat flux estimates that match experimental values in the stationary state (Table 4), the average emissive power values are noticeably different between models. Nevertheless, it should be noted that since E_b was determined from Eq. (4), the ratio between E_b and E_s does not vary across all cases. This means that the methodology can be extended to other operational conditions (type of fuel and pool diameter), in which other models for the estimation of E_s might be considered more appropriate.

Fig. 2 shows the evolution of the ratio between emissive power in the boilover and stationary periods and the pool diameter; a lesser increase in emissive power is observed when the dimension of the fire is increased. This can occur for two reasons: on the one hand, the fuel left to be burned at boilover decreases with diameter [13] and less fuel can therefore be dragged into the flame by the vapour. On the other hand, the bigger the fire the more difficult it is for air to penetrate the flame and it will rarely reach the centre of the fire; thus, the increase in fire turbulence produced by boilover is much more efficient for small diameters, as shown in Table 5.

Table 5
Average emissive power values, for every pool diameter, during both stationary and boilover period

D (m)	Model 7		Model 8		Model 9		Model 10		Ratio
	E_s (kW/m^2)	E_b (kW/m^2)	E_s (kW/m^2)	E_b (kW/m^2)	E_s (kW/m^2)	E_b (kW/m^2)	E_s (kW/m^2)	E_b (kW/m^2)	
1.5	37.60	73.17	25.13	48.89	56.37	109.70	40.00	77.84	1.95
3	36.42	60.28	36.32	60.12	54.79	90.71	50.04	82.83	1.66
4	34.86	49.38	39.92	56.56	53.77	76.16	56.36	79.84	1.42
5	33.93	47.49	36.70	51.37	52.76	73.84	62.99	88.16	1.40
6	32.46	43.22	32.90	43.81	51.77	68.93	59.43	79.14	1.33

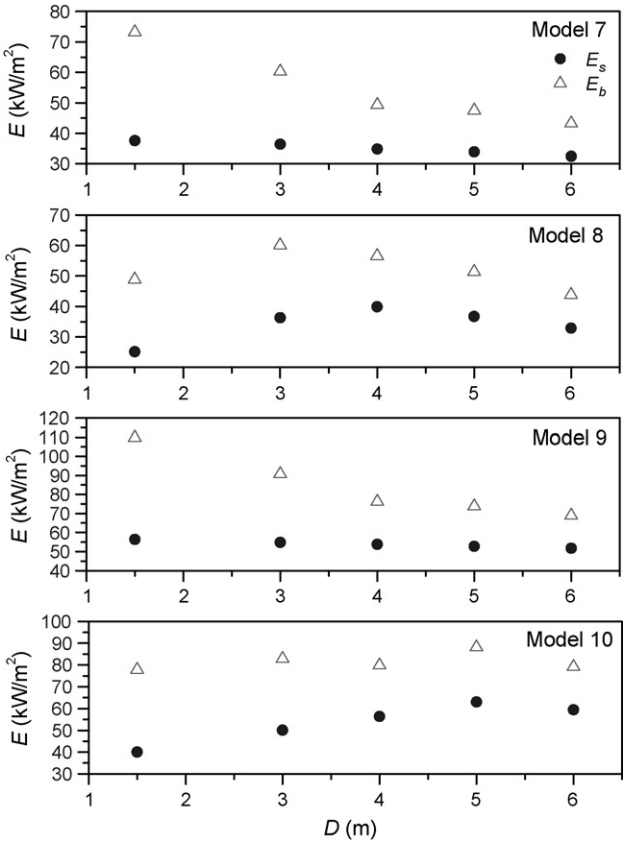

Fig. 3. Graphical representation of the determined values of average emissive power as a function of the diameter.

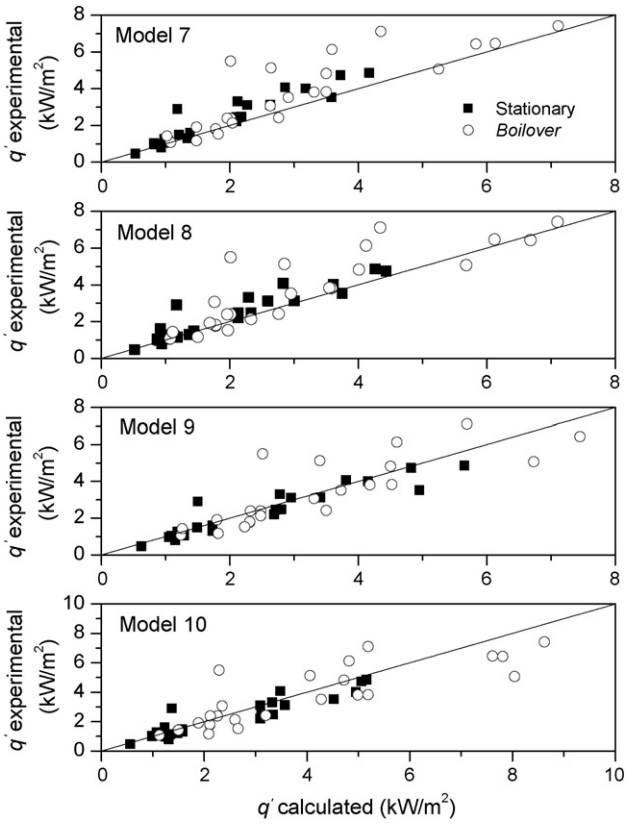

Fig. 4. Comparison between the experimental and calculated data of incident heat flux.

In order to decide which of the four models is more appropriate for determining the necessary increase in safety distances, the following analyses were performed:

- The values of average emissive power were represented graphically against the pool diameter, both for stationary and boilover phases, in order to establish which model presents an evolution representative of a real scenario (Fig. 3).
- For all models, the experimental and predicted heat flux data were compared graphically and numerically. The results are shown in Fig. 4 and Table 6, where accuracy was again assessed using the NMSE and FB parameters.

The following conclusions were reached:

- Models 9 and 10 provide more accurate values of NMSE and FB.
- The correlations of emissive power made by E-REW_MOD and E-SHOKRI give values for the stationary period that consistently decrease with diameter. However, recent studies including [6] have demonstrated that the emissive power in diesel-oil and gasoline fires grows slightly with pool size until a certain diameter and then decreases rapidly. The initial increase is caused by the rise in flame temperature with the dimension of the fire. Nevertheless, as the diameter of the fire/pool increases, smoke production becomes increasingly significant and generates a well-known effect by which the smoke blocks the emitted radiation. A combination of these two effects leads to the evolution described above. The equations for emissive power given by E-FRAC_RAD and E-MUÑOZ therefore appear more appropriate, as they consider the mechanism described.
- Models 7 and 8, since they disregard the influence of atmospheric transmissivity (τ is always equal to 1), give smaller emissive values, which leads to an underestimation of the heat

Table 6
Accuracy of the predictions of incident heat fluxes, both for stationary and boilover

Model	E	τ	Stationary		Boilover	
			NMSE	FB	NMSE	FB
7	E-REW_MOD	1	0.077	0.180	0.104	0.154
8	E-FRAC_RAD	1	0.073	0.137	0.101	0.126
9	E-SHOKRI	Bagster and Pitblado [16]	0.044	−0.064	0.081	−0.074
10	E-MUÑOZ	Bagster and Pitblado [16]	0.065	−0.076	0.102	−0.085

flux in proximity to the fire. Conversely, models 9 and 10 give higher heat flux values at these distances and only underestimate radiation at points located comparatively far from the fire, which are of no interest in a study of safety distances.

- Finally, the emissive power during boilover estimated in model 10 is practically constant with pool diameter. This is quite plausible if we consider that the smoke decrease during boilover is the smaller the bigger the diameter, due to the difficulty of air penetration [19]. It is reasonable to assume, therefore, that the average emissive power of the flame during water ebullition will not depend excessively on diameter, but will have a maximum value corresponding to the emissive power of the external surface of the flame.

Our interpretation of the analysis performed suggests that model 10 is the most suitable for determining the required increase in safety distances, since it gives a clearer illustration of emissive power evolution, both for the stationary and boilover periods.

3.3. Safety distances

The results from model 10 were used to estimate the increase in safety distances required during boilover. Wind speeds ranging from 0 to 1.5 m/s, an ambient temperature of 20 °C and a relative humidity of 50% were employed. The value of the heat flux limit for a possible *domino effect* was set at 8 kW/m^2, in accordance with to Spanish legislation [20].

The formulae proposed in [19] were used for flame length and tilt estimation. It should be noted that the correlation for flame tilt determination presupposes that the flame is tilted only at values of u^* greater than 1. The adimensional wind speed u^*, as shown in Eqs. (7) and (8), depends on the burning rate, meaning that the stationary and boilover periods can give different values of u^* even with the same wind speed.

$$u^* = \frac{u}{u_c} \tag{7}$$

$$u_c = \left(\frac{g\dot{m}D}{\rho_a}\right)^{1/3} \tag{8}$$

This implies that the flame is considered tilted for different wind speeds. Table 7 shows the limits below which the flame can be considered straight in the two characteristic phases of the fire and the required increase in safety distances during boilover. It can be clearly observed that safety distances must be increased further for smaller diameters, due to a greater increase in emissive power.

Table 7
Safety distances for straight flames and wind speed limits

D (m)	u (m/s)		x_c (m)		Ratio
	Stationary	Boilover	Stationary	Boilover	
1.5	0.75	0.90	2.58	4.29	1.66
3	1.05	1.05	5.29	7.74	1.46
4	1.05	1.05	7.25	9.50	1.31
5	1.20	1.05	9.40	12.17	1.29
6	1.35	1.05	10.50	13.13	1.25

Table 8
Safety distances for a 1.5 m fire

u (m/s)	u^*		x_c (m)		Ratio
	Stationary	Boilover	Stationary	Boilover	
<0.75	<1.00	<1.00	2.58	4.29	1.66
1.20	1.54	1.24	3.65	5.30	1.45
1.35	1.73	1.39	3.74	5.32	1.42
1.50	1.92	1.55	3.80	5.30	1.39

Table 9
Safety distances for a 4 m fire

u (m/s)	u^*		x_c (m)		Ratio
	Stationary	Boilover	Stationary	Boilover	
1.05	0.89	0.95	7.25	9.50	1.31
1.20	1.02	1.09	9.14	11.86	1.30
1.35	1.15	1.23	9.43	11.94	1.27
1.50	1.27	1.36	9.65	11.98	1.24

When wind speed exceeds such limits, it can generally be stated that the higher the wind speed the smaller the increase required in safety distances, as Tables 8 and 9 show for fires of 1.5 and 4 m, respectively. This behaviour is consistent with the fact that flame length decreases more rapidly with wind speed during boilover than in the stationary period [19].

The analysis performed therefore showed that, should boilover occur, safety distances must be increased with respect to the stationary period, with or without wind. According to Table 7, when wind speed is negligible, this increase must be greater than 65% for the small diameters (1.5 m) and between 25 and 30% with respect to the stationary for diameters of more than 6 m.

It should be noted that the model presented here was developed for diesel-oil fires in the case of boilover and is therefore difficult validate with previous experimental data, since little information is available. Nevertheless, as we have mentioned, experiments performed in Japan with 30 mm of crude oil [7] produced similar radiation intensity data ($I_{b,rad}$) to our own results, suggesting that the increases in safety distances presented in this work may also be suitable for other fuels.

4. Conclusions

The study of the thermal hazards of pool fires during boilover led to the following considerations:

1. Radiation intensity – the boilover effect on the radiation emitted by the flame and received by a target at a certain distance from the pool – decreases according to the thickness of fuel at the onset of the phenomenon.
2. Emissive power during boilover increases as expected, due to a reduction in smoke production. The effect is smaller when the pool diameter is greater, since less fuel is left to be burned at the onset of boilover and it is harder for air to penetrate.

3. Using experimental data for heat flux increase during boilover, the most common models for predicting flame radiation in the stationary were modified, in order to also predict thermal radiation during the water ebullition phase.
4. In our opinion, the model proposed by Muñoz, combined with the formula devised by Bagster and Pitblado for predicting atmospheric transmissivity, is the most appropriate when trying to predict the necessary increase in safety distances in pool fires that could involve boilover.
5. According to our results, the increase in safety distances must be greater than 65% for the small diameters (1.5 m) and between 25 and 30% with respect to the stationary for diameters of more than 6 m.

Acknowledgements

This work is sponsored by the Ministry of Science and Technology Commission (Project CTQ2005-06231). The authors also would like to acknowledge REPSOL Petróleo, S.A. for their financial support.

References

[1] M. Shokri, C.L. Beyler, Radiation from large pool fires, SFPE J. Fire Protect. Eng. 1 (4) (1989) 141–150.
[2] K.S. Mudan, Thermal radiation hazards from hydrocarbon pool fires, Prog. Energ. Combust. 10 (1984) 59–80.
[3] P.J. Rew, W.G. Hulbert, Development of Pool Fire Thermal Radiation Model, HSE Contract Research Report No. 94, 1996.
[4] P.J. Rew, W.G. Hulbert, D.M. Deaves, Modelling of thermal radiation from external hydrocarbon pool fires, Transact. IChemE, Part B 75 (1997) 81–89.
[5] C.J.H. Van Den Bosch, R.A.P.M. Weterings, Methods for the Calculation of Physical Effects Due to Releases of Hazardous Materials (Liquid and Gases) (a.k.a. TNO Yellow Book), 3rd ed., Committee for the Prevention of Disasters, The Hague, The Netherlands, 1997.
[6] M.A. Muñoz, Estudio de los parámetros que intervienen en la modelización de los efectos de grandes incendios de hidrocarburos: geometría y radiación térmica de la llama, PhD Tesis, Chemical Engineering Department, Universitat Politècnica de Catalunya, Barcelona, 2005.
[7] H. Koseki, Boilover and crude oil fire, J. Appl. Fire Sci. 3 (3) (1994) 243–272.
[8] B. Kozanoglu, F. Ferrero, M. Muñoz, J. Arnaldos, J. Casal, Velocity of the convective currents in boilover, Chem. Eng. Sci. 61 (8) (2006) 2550–2556.
[9] M. Arai, K. Saito, R.A. Altenkirch, A study of boilover in liquid pool fires supported on water. Part I. Effects of a water sublayer on pool fires, Combust. Sci. Technol. 71 (1990) 25–40.
[10] J.P. Garo, J.P. Vantelon, Thin layer boilover of pure or multicomponet fuels, Prev. Hazard. Fires Explos. (1999) 167–182.
[11] J.P. Garo, P. Gillard, J.P. Vantelon, A.C. Fernandez-Pello, Combustion of liquid fuels spilled on water. Prediction of time to start of boilover, Combust. Sci. Technol. 147 (1999) 39–59.
[12] H. Hasegawa, Experimental study on the mechanism of hot zone formation in open-tank fires, in: Proceedings of the Second International Symposium on Fire Safety Science, 1987, pp. 221–230.
[13] F. Ferrero, M. Muñoz, B. Kozanoglu, J. Casal, J. Arnaldos, Experimental study of thin-layer boilover in large-scale pool fires, J. Hazard. Mater. 137 (3) (2006) 1293–1302.
[14] J.M. Chatris, J. Quintela, J. Folch, E. Planas, J. Arnaldos, J. Casal, Experimental study of burning rate in hydrocarbon pool fires, Combust. Flame 126 (2001) 1373–1383.
[15] M. Muñoz, J. Arnaldos, J. Casal, E. Planas, Analysis of the geometric and radiative characteristics of hydrocarbon pool fires, Combust. Flame 139 (2004) 263–277.
[16] D.F. Bagster, R.M. Pitblado, Thermal hazards in the process industry, Chem. Eng. Prog. (1989) 69–75.
[17] F.D. Wayne, An economical formula for calculating atmospheric infrared transmissivities, J. Loss Prevent. Proc. 4 (2) (1991) 86–92.
[18] J. Casal, H. Montiel, E. Planas, J.A. Vilchez, Análisis del riesgo en instalaciones industriales, Edicions UPC, Barcelona, 1999.
[19] F. Ferrero, M. Muñoz, J. Arnaldos, Effects of thin-layer boilover on flame geometry and dynamics in large hydrocarbon pool fires, Fuel Process. Technol. (2006), in press.
[20] Real Decree 1196/2003 of September 19 (BOE no. 242 of October 9, 2003).